

Leveraging Auto-Distillation and Generative Self-Supervised Learning in Residual Graph Transformers for Enhanced Recommender Systems

Eya Mhedhbi¹, Youssef Mourchid²[0000-0003-4108-4557], and Alice Othmani^{3,1}[0000-0002-3442-0578]

¹ Declic AI Research mhedhbiaya99@gmail.com

² CESI LINEACT Laboratory, UR 7527, Dijon, France ymourchid@cesi.fr

³ Université Paris-Est, LISSI, UPEC, 94400 Vitry sur Seine, France

Corresponding author: alice.othmani@u-pec.fr

Abstract. This paper introduces a cutting-edge method for enhancing recommender systems through the integration of generative self-supervised learning (SSL) with a Residual Graph Transformer. Our approach emphasizes the importance of superior data enhancement through the use of pertinent pretext tasks, automated through rationale-aware SSL to distill clear ways of how users and items interact. The Residual Graph Transformer incorporates a topology-aware transformer for global context and employs residual connections to improve graph representation learning. Additionally, an auto-distillation process refines self-supervised signals to uncover consistent collaborative rationales. Experimental evaluations on multiple datasets demonstrate that our approach consistently outperforms baseline methods.

Keywords: Recommender Systems · Generative Self-Supervised learning · Residual Graph Transformer · Masked Autoencoder · Representation Learning.

1 Introduction

In today's age of information overload, recommender systems are essential for offering personalized suggestions for items that users might find appealing, such as products on e-commerce platforms[1] and social media[2]. These systems are integral to enhancing user engagement and facilitating discovery amid vast content repositories like Amazon, Alibaba, Facebook, YouTube, and TikTok.

Collaborative filtering (CF) is widely employed within these systems, it generates suggestions by leveraging the preferences of similar users or items to recommend new items for a given user[3]. In recent years, graphs have been extensively utilized in a variety of applications [4], with Graph Neural Networks (GNNs) enhancing collaborative filtering by modeling users and items as connected nodes. Models like PinSage [5], NGCF [6], and LightGCN [7] use GCNs

for better embeddings and accuracy. LightGCN [7] focuses on structural signals, while GNNs face challenges with sparse and noisy data. Self-supervised learning (SSL), a powerful technique that trains models using unlabeled data, has emerged as a valuable approach in recommender systems by learning from unlabeled data. SSL methods are either contrastive, like SGL [8], which creates varied views of interaction graphs, or generative, like GFormer [9], which reconstructs masked interactions. Graph Contrastive Learning (GCL) is useful but struggles with noise. Traditional methods, such as hypergraph-based passing (HCCF) [10] and node clustering (NCL) [11], address some issues but are also noise-prone.

Generative Learning [12] in recommendation systems involves generating new data instances from existing ones. Self-supervised collaborative filtering leverages this approach through several advanced techniques: (1) Variational Autoencoders (VAE): Methods like CaD-VAE [13] enhance modeling by integrating item content, optimizing hyperparameters, and using advanced frameworks to improve efficiency. (2) Masked Autoencoders: Techniques such as AutoCF [14] and GFormer [9] reconstruct data by focusing on significant user-item interactions. GFormer emphasizes autonomous edge detection and reconstruction using user and item representations. (3) Denoised Diffusion Models: Approaches like DiffRec [15] use diffusion models to reduce noise from user ratings or latent variables, enhancing prediction accuracy and efficiency.

To overcome the limitations of the different approaches and in order to leverage the strengths of various techniques, we propose a novel recommender system called Residual Graph Transformer. It automatically extracts self-supervised signals, improves the graph autoencoder with adaptive methods, and uses Transformers to capture relationships and collaborative patterns for better recommendations. Auto-distillation is also used to improve the performance. Our main contributions can be summarized as follows:

- We introduce automated ways to enhance data through self-supervised learning (SSL) and explain how these methods can make recommendations more robust.
- We use graph transformer models with residual connections and light self-attention to identify consistent data patterns. Auto-distillation boosts recommendation performance, and a graph autoencoder enhances the representation of user-item interactions.
- We evaluate our proposed model on multiple datasets and find it consistently outperforms other methods in various scenarios.

The organization of the rest of this paper is as follows. Section 2 comprehensively details different components of our proposed model. Section 3 outlines the experimental setup and presents the results. Finally, concluding remarks are presented in Section 4.

2 Proposed Approach

2.1 Problem Formulation

In this work, we consider a recommendation system with I users $U = \{u_1, u_2, \dots, u_I\}$ and J items $P = \{p_1, p_2, \dots, p_J\}$. The user interactions are captured by an interaction matrix $A \in R^{I \times J}$, where $a_{i,j} = 1$ indicates an interaction between user u_i and item p_j , and $a_{i,j} = 0$ otherwise. To convert the interaction matrix into an interaction graph for graph-based CF, we define a graph $G = \{V, E\}$, where $V = U \cup P$ represents the set of nodes, and $E = \{e_{i,j} | a_{i,j} = 1\}$ denotes the set of edges corresponding to user-item interactions. With these definitions, the graph-based CF can be represented as a prediction function for user-item interactions: $\hat{y}_{i,j} = f(G; \Theta)$, where $\hat{y}_{i,j}$ is the predicted score for the unknown interaction between user u_i and item p_j , and Θ represents the model parameters.

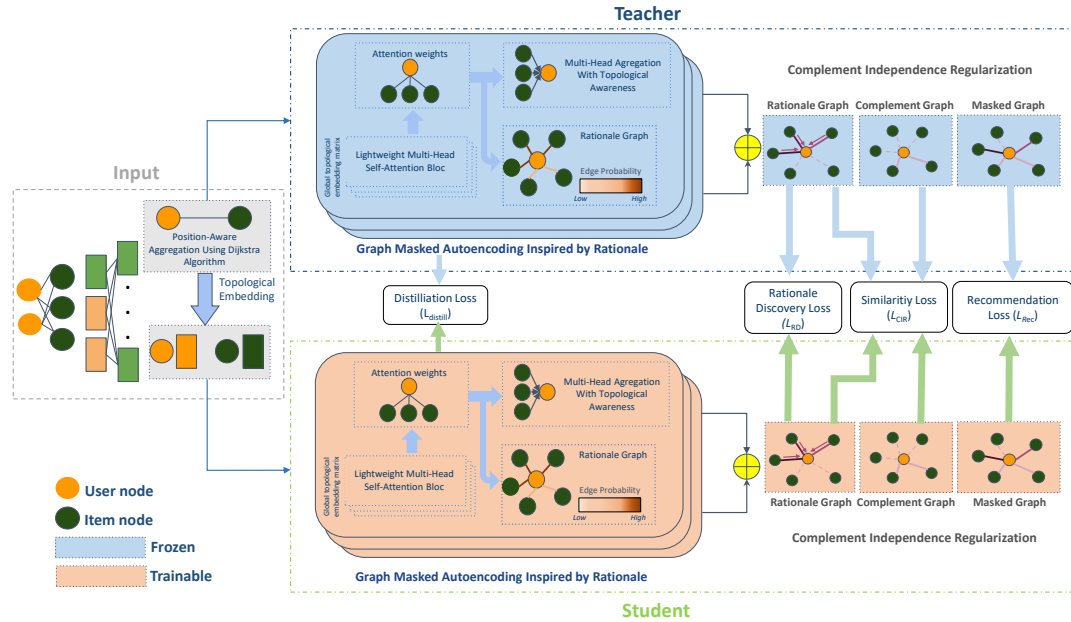


Fig. 1: Overall framework illustration of our proposed approach. The figure is better seen zoomed in the digital version of the document.

2.2 Integration of Global Topology Information

Inspired by the efficiency of position-aware graph neural networks (P-GNNs) [16] in capturing comprehensive relational information on a global scale, we initially

select a subset of anchor nodes $V_A \subset V$ from the user-item interaction graph $G = \{V, E\}$. We then compute the distance between a target node v_k and the anchor sets v_a using Dijkstra’s algorithm. Given the calculated distances, we compute the correlation weight, denoted as $\omega_{k,a}$, for each pair of target-anchor nodes (k, a) . The correlation weight is defined as follows:

$$\omega_{k,a} = \begin{cases} \frac{1}{d_{k,a}+1} & \text{if } d_{k,a} \leq q \\ 0 & \text{otherwise.} \end{cases} \quad (1)$$

q is the upper limit for the correlation weight between any target and anchor node. This method ensures that only nodes within a certain distance contribute to the target node’s embedding, effectively capturing the positional relationships within the graph. Dijkstra’s algorithm is used for a more accurate representation of these relationships, resulting in more informative node embeddings. This holds true even when edge weights are binary, Dijkstra’s algorithm can provide a more nuanced understanding of the graph structure, which can lead to improved performance. The correlation weights of the nodes are normalized to a range of $[0, 1]$. Using the weight $\omega_{k,a}$, the target node embedding is refined by considering the correlation weights between the target node k and each anchor node $v_a \in V_A$: $\tilde{h}_k^l = \sum_{v_a \in V_A} W^l \cdot \omega_{k,a} \cdot [\tilde{h}_k^{l-1} || \tilde{h}_a^{l-1}] / |V_A|$

Here, \tilde{h}_k^l and $\tilde{h}_k^{l-1} \in R^d$ denote the embeddings of node v_k in the l -th and $(l-1)$ -th graph propagation layer, respectively. To capture the global topological context based on anchor nodes, H_T^l is defined as the global topological embedding matrix in the l -th layer. $W^l \in R^{d \times 2d}$ represents a learnable transformation matrix. After L graph information propagation steps, the embeddings in \tilde{H}^L retain the high-order topological information. This information is then injected into the id-corresponding embeddings to produce the topological embeddings:

$$\bar{H} = TE(H; \{W_T^l\}) \quad (2)$$

In this manner, our parameterized rationale generator can capture global collaborative relationships and uncover informative interaction patterns between users and items for SSL augmentation.

2.3 Residual Graph Transformer-Based Collaborative Rationale Discovery

Rational discovery helps to find useful patterns in how users interact with items. These patterns can help improve recommendation systems in changing environments, even when there are few labels for supervision. We propose an advanced method for extracting these rationales using our Graph Transformer model with residual connections. Our method is inspired by the core self-attention mechanisms of the Transformer architecture, focusing on invariant user preference information for robust generative self-supervision. This approach mitigates noise and biases in observational behavior data, enhancing recommendation performance. The core of our method is a rationale discovery module within a graph

transformer framework, encoding node-wise relations as selected rationales and incorporating the positional information of user and item nodes. We leverage global topology-aware node embeddings, \bar{H} , in a multi-head self-attention mechanism for the rationalization process. The correlation between nodes v_k and $v_{k'}$ for the h -th attention head is computed as:

$$\alpha_{k,k'}^h = \frac{\exp(\tilde{\alpha}_{k,k'}^h)}{\sum_{k'} \exp(\tilde{\alpha}_{k,k'}^h)}; \tilde{\alpha}_{k,k'}^h = \frac{(W_Q^h \cdot \bar{h}_k)^T \cdot (W_K^h \cdot \bar{h}_{k'})}{\sqrt{d/H}} \quad (3)$$

Here, $\alpha_{k,k'}^h$ represents the normalized attention score between nodes v_k and $v_{k'}$ for the h -th attention head, and $\tilde{\alpha}_{k,k'}^h$ is the raw attention score before normalization. W_Q^h and W_K^h in $\mathbb{R}^{d_H \times d}$ are the transformations used to derive the query and key embeddings for calculating the attention scores. As the attention scores encoded by our graph transformer reflect the strength of node-wise dependencies, we aggregate the multi-head scores to obtain the probability scores, $p((v_k, v_{k'})|G)$, of graph edges, such as $(v_k - v_{k'})$, being selected as rationales. These rationales represent a subset of crucial user-item interaction patterns that most effectively highlight the user preference learning process with consistent representations, as shown:

$$\bar{p}((v_k, v_{k'})|G) = \frac{\bar{\alpha}_{k,k'}}{\sum_{(v_k, v_{k'}) \in E} \bar{\alpha}_{k,k'}}; \bar{\alpha}_{k,k'} = \frac{\sum_{h=1}^H \alpha_{k,k'}^h}{H} \quad (4)$$

To sample a rationale estimated by our topology-aware graph transformer, we individually select $\rho_R \cdot |E|$ edges from the edge set E based on their probability scores, $p((v_k, v_{k'})|G)$. Here, the hyperparameter $\rho_R \in R$ determines the proportion of important edges chosen for rationalization. To improve our model, we added a residual operation to our residual graph transformer. This upgrade builds on the basic graph transformer by repeatedly applying it and combining the results through a residual link. This helps maintain the flow of gradients during training, making learning more efficient and improving the model’s performance. This residual modification significantly boosts the model’s ability to find and understand important patterns in user-item interactions, enhancing recommendation effectiveness in changing environments with limited supervised data. In addition to the above, we have also incorporated a streamlined version of self-attention, into our model. This version employs linear layers for transforming the input vectors, which facilitates easier initialization and improved gradient propagation. An output projection layer has been integrated to transform the resulting embeddings back to the original dimensionality. This makes the Light Self-Attention particularly suitable for large datasets and deep architectures, while being more computationally and memory efficient.

2.4 Self-Augmentation with Rationale Awareness

Integrating Rationales into Graph Masked Autoencoding. The approach uses a graph-masked autoencoder for self-augmentation, leveraging collaborative

rationales. The rationale-aware mask autoencoder masks identified rationales from the interaction graph, allowing for effective reconstruction. The masked graph structure $G_M = \{V, E_M\}$ is created by inverting the rationale scores. The masked graph maintains a higher edge density than the rationale graph, ensuring only the most significant rationale edges are removed, promoting noise-resistant autoencoding. The process begins with the following operation:

$$S = GT(G_M, TE(\bar{S}_L)); \bar{s}_l = \sum_{(v_k, v_{k'}) \in E_M} \beta_{k, k'} \cdot \bar{s}_{l_{1_{k'}}} \quad (5)$$

Here, $GT()$ and $TE()$ represent the graph transformer network and the topological information encoder, respectively. \bar{s}_l is the sum of the product of $\beta_{k, k'}$ and $\bar{s}_{l_{1_{k'}}$ for all edges in E_M . This equation is used to enhance the initial embeddings with L -order local node embeddings \bar{S}_L , encoded from LightGCN. The embeddings S are then used to train the reconstruction of the masked user-item interactions. The final embeddings $S \in R^{(I+J) \times d}$ in the autoencoder are utilized for training the reconstruction of the masked user-item interactions, and for computing the masked autoencoder loss L_{MAE} , which is defined as follows:

$$L_{MAE} = \sum_{(v_k, v_{k'}) \in E \setminus E_M} -\tilde{y}_{k, k'}; \tilde{y}_{k, k'} = s_k^\top s_{k'} \quad (6)$$

This loss is specifically designed for reconstructing masked interaction patterns, $\tilde{y}_{k, k'}$ represents the predicted scores for the edge $(v_k, v_{k'})$ on graph G . The reconstruction process is enhanced by encoding local node embeddings from LightGCN into the initial embeddings, ensuring effective reconstruction of key interaction patterns adaptable to downstream recommendation tasks. This approach helps prevent noise in the generative self-supervised learning process.

Modeling Complement Independence. To make the rationale discovery process more independent and reduce redundancy, we use a learning technique called contrastive regularization. This minimizes the mutual information between the rationale graph G_R and a complement graph G_C . We create the complement graph G_C by sampling edges with a low rate $\rho_C \ll \rho_M$ to focus on noisy edges. The edges of the complement graph (E_C) are generated as follows:

$$E_C \sim p_C(E_C|G) = \rho_M(E_C|G); |E_C| = \rho_C \cdot |E| \quad (7)$$

This is similar to graph masking but with a smaller sampling rate. Then, we used the loss function \mathcal{L}_{CIR} , to reduce the similarities between the rationale graph G_R and the complement graph G_C in high-order representations, which can be defined as follows:

$$\mathcal{L}_{CIR} = \log \sum_{v_k \in V} \exp \left(\frac{\cos(e_k^R, e_k^C)}{\tau} \right) \quad (8)$$

Here, e_k^R and e_k^C are the embeddings of node k in the rationale graph and complement graph, respectively. The cosine similarity between these embeddings is

divided by a temperature coefficient τ , and the exponential sum of these values across all nodes is taken. This loss function ensures that the embeddings of the rationale graph and the complement graph are pushed apart, enhancing the model’s ability to separate useful information from noise.

SSL-Augmented Model Optimization. During training, we use embeddings $S \in R^{(I+J) \times d}$ to predict interactions for training the recommender system. The point-wise loss function L_{Rec} is minimized as follows:

$$L_{Rec} = \sum_{i,j=1}^A -\log \left(\frac{\exp(s_i^T s_j)}{\sum_{p' \in P} \exp(s_i^T s_{p'})} \right) \quad (9)$$

Our Model maximizes predictions for all positive user-item interactions and contrasts by minimizing predictions for negative interactions. During testing, we substitute the masked graph G_M with the observed interaction graph G and predict user u_i ’s relation to item p_j as $\hat{y}_{i,j} = s_i^T s_j$.

2.5 Auto Distillation Graph

Auto-distillation improves model training by using a single model as both teacher and student. After steps like negative sampling and embedding generation, the model’s embeddings (user, item, and graph structure) are used to train a second model, the distillation model. The distillation model learns to mimic the main model’s outputs, guided by a loss function, Mean Squared Error (MSE), which reduces differences between the outputs of the main model and the distillation model. This process can be expressed as:

$$L_{\text{distill}} = \text{MSE}(h_u^{\text{student}}, h_u^{\text{teacher}}) + \text{MSE}(h_i^{\text{student}}, h_i^{\text{teacher}}) \\ + \text{MSE}(h_c^{\text{student}}, h_c^{\text{teacher}}) + \text{MSE}(h_s^{\text{student}}, h_s^{\text{teacher}}) \quad (10)$$

where h_u^{student} and h_u^{teacher} represent the user embeddings generated by the student and teacher models, respectively, h_i^{student} and h_i^{teacher} represent the item embeddings, h_c^{student} and h_c^{teacher} represent the contrastive list embeddings, and h_s^{student} and h_s^{teacher} represent the subgraph list embeddings.

2.6 Our Objective Loss

The BPR loss, L_{RD} , guides rationale discovery by optimizing the model’s objective for the downstream task:

$$L_{RD} = \sum_{(u_i, p_j^+, p_j^-)} -\log \text{sigm}(\bar{y}_{i,j+} - \bar{y}_{i,j-}) \quad (11)$$

Here, a triplet of user u_i and items p_j^+, p_j^- is sampled such that $(u_i, p_j^+) \in E$ and $(u_i, p_j^-) \notin E$. The sigmoid function, $\text{sigm}(\cdot)$, models the probability that the positive interaction p_j^+ is preferred over p_j^- .

In our model, the total loss function L integrates several key objectives: L_{Rec} , L_{RCS} , L_{RD} , L_{CIR} , and the Frobenius norm regularization $\|\Theta\|_F^2$. Additionally, the distillation loss L_{distill} refines the model’s internal representations over training epochs, enhancing the accuracy of recommendations. The overall objective L to be minimized during training consolidates these components:

$$L = L_{\text{Rec}} + \lambda_{\text{distill}} L_{\text{distill}} + \lambda_1 \cdot L_{\text{RD}} + \lambda_2 \cdot L_{\text{CIR}} + \lambda_3 \cdot \|\Theta\|_F^2 \quad (12)$$

Here, λ_1 , λ_2 , λ_3 , and λ_{distill} are hyperparameters balancing the impact of each loss term. The Frobenius norm regularization $\|\Theta\|_F^2$ helps keep the model stable by limiting parameter values. This approach balances reconstruction, rationale discovery, and regularization for better optimization in recommendation systems.

3 Experiments and results

3.1 Experimental Settings

Datasets. We use three real-world datasets to assess the performance of our proposed model. These include the Yelp dataset, which focuses on recommending business venues from the renowned Yelp platform; the Ifashion dataset, a collection of fashion outfit data gathered by Alibaba, and the LastFM dataset, which records user interactions within music applications and internet radio platforms. The characteristics and statistics of these datasets are detailed in Table 1.

Table 1: Statistics of the experimental datasets

| Dataset | Users | Items | Interactions | Density |
|----------|--------|--------|--------------|-------------|
| Yelp | 42,712 | 26,822 | 182,357 | $1.6e^{-4}$ |
| Ifashion | 31,668 | 38,048 | 618,629 | $5.1e^{-4}$ |
| LastFM | 1,889 | 15,376 | 51,987 | $1.8e^{-3}$ |

Evaluation Protocols. For each dataset, interactions are split into training, validation, and test sets with a division ratio of 70%, 5%, and 25%, respectively. To evaluate the effectiveness of our proposed model, we employ a comprehensive all-rank evaluation method that mitigates potential biases from negative sampling. The performance of the models is assessed using two key metrics: Recall Ratio (Recall@K) and Normalized Discounted Cumulative Gain (NDCG@K) for $K = 10, 20, 40$. NDCG is calculated using the formula:

$$NDCG@k = \frac{DCG@k}{IDCG@k} \quad (13)$$

Where $DCG@k$ is the Discounted Cumulative Gain at position k , calculated by summing the gains of the recommendations up to position k and giving more weight to higher-ranked recommendations, and $IDCG@k$ is the Ideal Discounted Cumulative Gain at position k , representing the optimal possible DCG when the recommendations are perfectly ranked.

3.2 Hyperparameter Settings

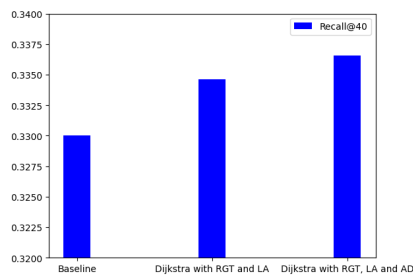
We used Weights & Biases (W&B)⁴ for hyperparameter tuning to maximize Recall and NDCG values. Table 2 presents the best hyperparameter combinations for the different datasets.

Table 2: The best hyperparameter combinations used across various datasets in our model.

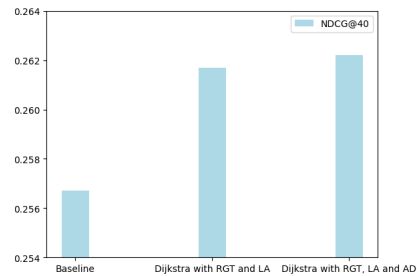
| Dataset | anchor | set | reg | lr | ssl | reg | GCN | B2 | PNN | Batch | ctra | GT | GTW | Head | latdim |
|----------|--------|-----|---------|-------|-----|-----|-----|----|------|--------|------|------|-----|------|--------|
| Yelp | 16 | | 0.0001 | 0.001 | 0.5 | 3 | 0.5 | 2 | 4096 | 0.005 | 2 | 0.05 | 2 | 64 | |
| Ifashion | 64 | | 0.00001 | 0.001 | 1.5 | 3 | 1 | 1 | 4096 | 0.0005 | 1 | 0.05 | 2 | 32 | |
| LastFM | 32 | | 0.0001 | 0.001 | 0.5 | 1 | 1 | 2 | 4096 | 0.005 | 1 | 0.1 | 8 | 64 | |

3.3 Ablation Study

To validate the effectiveness of our contributions, we conducted an ablation study comparing three versions of our model using the LastFM dataset. The first version, Graph Transformer, served as our baseline model. We then added Dijkstra’s algorithm and the Residual Graph Transformer(RGT) with light attention(LA) in the second version, followed by the application of auto-distillation in the third version(AD). As shown in Fig. 2, each enhancement led to progressive improvements in Recall@40 and NDCG@40 metrics, underscoring the effectiveness of our proposed methods.



(a) LastFM Dataset - Recall@40



(b) LastFM Dataset - NDCG@40

Fig. 2: Effect of different components of our proposed models on LastFM dataset in terms of Recall@40 and NDCG@40

Additionally, as mentioned in Fig. 3, we assess the impact of individual loss components on model performance, we conducted an ablation study by

⁴ <https://wandb.ai/site>

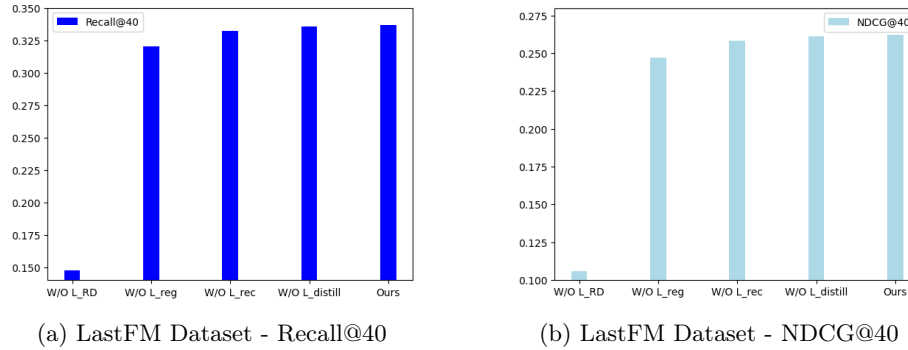


Fig 3: Effect of different losses used in our model on the Recall@40 and NDCG@40 metrics for the LastFM dataset

sequentially removing each component and measuring changes in Recall@40 and NDCG@40. Results show that the L_RD component is crucial for guiding rationale discovery and optimizing the model, with its removal leading to significant drops in both metrics. The L_rec component is also vital, as its absence results in a major performance decline. The L_distill component, while less critical, still provides a positive but modest contribution. The L_reg component is essential for preventing overfitting, as indicated by the performance decrease when it is removed. Overall, the full model with all loss components included demonstrates the highest performance, underscoring the effectiveness of the combined loss strategy.

Table 3: Performance comparison between our proposed approach and all baselines on Ifashion, Yelp, LastFM datasets.

| Datasets | Metric | BiasMF | NCF | AutoRec | PinSage | NGCF | GCCF | LightGCN | EGLN | SLRec | NCL | HCCF | SGL | GFormer | Ours |
|----------|-----------|--------|--------|---------|---------|--------|--------|----------|--------|--------|--------|--------|--------|---------|---------------|
| Ref | — | [17] | [3] | [18] | [5] | [6] | [19] | [7] | [20] | [21] | [11] | [10] | [8] | [9] | — |
| Yelp | Recall@10 | 0.0122 | 0.0166 | 0.0230 | 0.0278 | 0.0438 | 0.0484 | 0.0422 | 0.0458 | 0.0418 | 0.0493 | 0.0518 | 0.0522 | 0.0562 | 0.0583 |
| | NDCG@10 | 0.0070 | 0.0101 | 0.0133 | 0.0171 | 0.0269 | 0.0296 | 0.0254 | 0.0278 | 0.0258 | 0.0301 | 0.0318 | 0.0319 | 0.0350 | 0.0363 |
| | Recall@20 | 0.0198 | 0.0292 | 0.0410 | 0.0454 | 0.0678 | 0.0754 | 0.0761 | 0.0726 | 0.0650 | 0.0806 | 0.0789 | 0.0815 | 0.0878 | 0.0911 |
| | NDCG@20 | 0.0090 | 0.0138 | 0.0186 | 0.0224 | 0.0340 | 0.0378 | 0.0373 | 0.0360 | 0.0327 | 0.0402 | 0.0391 | 0.0410 | 0.0442 | 0.0458 |
| | Recall@40 | 0.0303 | 0.0442 | 0.0678 | 0.0712 | 0.1047 | 0.1163 | 0.1031 | 0.1121 | 0.1026 | 0.1192 | 0.1244 | 0.1249 | 0.1328 | 0.1377 |
| | NDCG@40 | 0.0117 | 0.0167 | 0.0253 | 0.0287 | 0.0430 | 0.0475 | 0.0413 | 0.0456 | 0.0418 | 0.0485 | 0.0510 | 0.0517 | 0.0551 | 0.0572 |
| Ifashion | Recall@10 | 0.0302 | 0.0268 | 0.0309 | 0.0291 | 0.0375 | 0.0373 | 0.0437 | 0.0473 | 0.0373 | 0.0474 | 0.0489 | 0.0512 | 0.0542 | 0.0555 |
| | NDCG@10 | 0.0281 | 0.0253 | 0.0264 | 0.0276 | 0.0350 | 0.0352 | 0.0416 | 0.0438 | 0.0353 | 0.0446 | 0.0464 | 0.0487 | 0.0520 | 0.0526 |
| | Recall@20 | 0.0523 | 0.0451 | 0.0537 | 0.0505 | 0.0636 | 0.0639 | 0.0751 | 0.0787 | 0.0633 | 0.0797 | 0.0815 | 0.0845 | 0.0894 | 0.0910 |
| | NDCG@20 | 0.0360 | 0.0306 | 0.0351 | 0.0352 | 0.0442 | 0.0445 | 0.0528 | 0.0549 | 0.0444 | 0.0558 | 0.0578 | 0.0603 | 0.0635 | 0.0650 |
| | Recall@40 | 0.0858 | 0.0785 | 0.0921 | 0.0851 | 0.1062 | 0.1047 | 0.1207 | 0.1277 | 0.1043 | 0.1283 | 0.1306 | 0.1354 | 0.1424 | 0.1435 |
| | NDCG@40 | 0.0474 | 0.0423 | 0.0483 | 0.0470 | 0.0585 | 0.0584 | 0.0677 | 0.0715 | 0.0582 | 0.0723 | 0.0744 | 0.0773 | 0.0818 | 0.0826 |
| LastFM | Recall@10 | 0.0609 | 0.0574 | 0.0543 | 0.0899 | 0.1257 | 0.1230 | 0.1490 | 0.1133 | 0.1175 | 0.1491 | 0.1502 | 0.1496 | 0.1573 | 0.1610 |
| | NDCG@10 | 0.0696 | 0.0645 | 0.0599 | 0.1046 | 0.1489 | 0.1452 | 0.1739 | 0.1263 | 0.1384 | 0.1745 | 0.1773 | 0.1775 | 0.1831 | 0.1886 |
| | Recall@20 | 0.0980 | 0.0956 | 0.0887 | 0.1343 | 0.1918 | 0.1816 | 0.2188 | 0.1823 | 0.1747 | 0.2196 | 0.2210 | 0.2236 | 0.2352 | 0.2385 |
| | NDCG@20 | 0.0860 | 0.0800 | 0.0769 | 0.1229 | 0.1759 | 0.1681 | 0.2018 | 0.1557 | 0.1613 | 0.2021 | 0.2047 | 0.2070 | 0.2145 | 0.2180 |
| | Recall@40 | 0.1450 | 0.1439 | 0.1550 | 0.1990 | 0.2794 | 0.2649 | 0.3156 | 0.2747 | 0.2533 | 0.3130 | 0.3184 | 0.3194 | 0.3300 | 0.3366 |
| | NDCG@40 | 0.1067 | 0.1055 | 0.1031 | 0.1515 | 0.2146 | 0.2049 | 0.2444 | 0.1966 | 0.1960 | 0.2437 | 0.2458 | 0.2498 | 0.2567 | 0.2622 |

3.4 Comparison with existing methods

We present the performance comparison between our proposed approach and several baseline methods on the Ifashion, Yelp, and LastFM datasets in Table 3. Our approach consistently surpasses the baselines across all datasets and metrics. For instance, on the Yelp dataset, our approach achieves the highest Recall@10 (0.0583) and NDCG@10 (0.0363), significantly surpassing the other models. Similar trends are observed in the Ifashion and LastFM datasets, where our model attains the best results in Recall and NDCG at various K values, with notable improvements in Recall@40 and NDCG@40. These results demonstrate the efficacy of our model, particularly the residual graph transformer and the automatic distillation strategies, which contribute to superior performance by efficient mining and leveraging collaborative rationales. Among these components, the topological graph position encoding and the multi-head self-attention mechanism are crucial, as they capture global context and enhance the understanding of user-item interactions.

4 Conclusion

This paper highlights how discovering meaningful user-item interaction patterns can improve collaborative filtering techniques through self-supervised learning. For that, we propose in this work a recommendation system that uses a residual graph transformer to automatically find hidden signals and coherent patterns. Our method includes topological graph position encoding for a global context and uses automatic distillation strategies to boost performance. Experiments show that our model outperforms several literature approaches across multiple datasets. In future work, we plan to explore advanced data augmentation techniques and expand our model to handle larger datasets and more diverse recommendation scenarios.

Acknowledgement

This work was supported by Declic, a deep tech startup. Declic is a social network for outings, meetings, and events, fostering genuine connections and shared activities in the real world (<https://declic.net/>)

References

1. Jianling Wang, Raphael Louca, Diane Hu, Caitlin Cellier, James Caverlee, and Liangjie Hong. Time to shop for valentine’s day: Shopping occasions and sequential recommendation in e-commerce. In *Proceedings of the 13th International Conference on Web Search and Data Mining*, pages 645–653, 2020.
2. Fanjin Zhang, Jie Tang, Xueyi Liu, Zhenyu Hou, Yuxiao Dong, Jing Zhang, Xiao Liu, Ruobing Xie, Kai Zhuang, Xu Zhang, et al. Understanding wechat user preferences and “wow” diffusion. *IEEE Transactions on Knowledge and Data Engineering*, 34(12):6033–6046, 2021.

3. Xiangnan He, Lizi Liao, Hanwang Zhang, Liqiang Nie, Xia Hu, and TS Chua. Neural collaborative filtering in: Proceedings of the 26th international conference on world wide web, 173–182. In *International World Wide Web Conferences Steering Committee*, 2017.
4. Youssef Mourchid and Rim Slama. Mr-stgn: Multi-residual spatio temporal graph network using attention fusion for patient action assessment. In *2023 IEEE 25th International Workshop on Multimedia Signal Processing (MMSP)*, pages 1–6. IEEE, 2023.
5. Rex Ying, Ruining He, Kaifeng Chen, Pong Eksombatchai, William L Hamilton, and Jure Leskovec. Graph convolutional neural networks for web-scale recommender systems. In *Proceedings of the 24th ACM SIGKDD international conference on knowledge discovery & data mining*, pages 974–983, 2018.
6. Xiang Wang, Xiangnan He, Meng Wang, Fuli Feng, and Tat-Seng Chua. Neural graph collaborative filtering. In *Proceedings of the 42nd international ACM SIGIR conference on Research and development in Information Retrieval*, pages 165–174, 2019.
7. Xiangnan He, Kuan Deng, Xiang Wang, Yan Li, Yongdong Zhang, and Meng Wang. Lightgcn: Simplifying and powering graph convolution network for recommendation. In *Proceedings of the 43rd International ACM SIGIR conference on research and development in Information Retrieval*, pages 639–648, 2020.
8. Jiancan Wu, Xiang Wang, Fuli Feng, Xiangnan He, Liang Chen, Jianxun Lian, and Xing Xie. Self-supervised graph learning for recommendation. In *Proceedings of the 44th international ACM SIGIR conference on research and development in information retrieval*, pages 726–735, 2021.
9. Chaoliu Li, Lianghao Xia, Xubin Ren, Yaowen Ye, Yong Xu, and Chao Huang. Graph transformer for recommendation. In *Proceedings of the 46th International ACM SIGIR Conference on Research and Development in Information Retrieval*, pages 1680–1689, 2023.
10. Lianghao Xia, Chao Huang, Yong Xu, Jiashu Zhao, Dawei Yin, and Jimmy Huang. Hypergraph contrastive collaborative filtering. In *Proceedings of the 45th International ACM SIGIR conference on research and development in information retrieval*, pages 70–79, 2022.
11. Zihan Lin, Changxin Tian, Yupeng Hou, and Wayne Xin Zhao. Improving graph collaborative filtering with neighborhood-enriched contrastive learning. In *Proceedings of the ACM web conference 2022*, pages 2320–2329, 2022.
12. Youssef Mourchid, Marc Donias, and Yannick Berthoumieu. Automatic image colorization based on multi-discriminators generative adversarial networks. In *2020 28th European signal processing conference (EUSIPCO)*, pages 1532–1536. IEEE, 2021.
13. Siyu Wang, Xiacong Chen, Quan Z Sheng, Yihong Zhang, and Lina Yao. Causal disentangled variational auto-encoder for preference understanding in recommendation. In *Proceedings of the 46th International ACM SIGIR Conference on Research and Development in Information Retrieval*, pages 1874–1878, 2023.
14. Lianghao Xia, Chao Huang, Chunzhen Huang, Kangyi Lin, Tao Yu, and Ben Kao. Automated self-supervised learning for recommendation. In *Proceedings of the ACM Web Conference 2023*, pages 992–1002, 2023.
15. Wenjie Wang, Yiyan Xu, Fuli Feng, Xinyu Lin, Xiangnan He, and Tat-Seng Chua. Diffusion recommender model. In *Proceedings of the 46th International ACM SIGIR Conference on Research and Development in Information Retrieval*, pages 832–841, 2023.

16. Jiaxuan You, Rex Ying, and Jure Leskovec. Position-aware graph neural networks. In *International conference on machine learning*, pages 7134–7143. PMLR, 2019.
17. Yehuda Koren, Robert Bell, and Chris Volinsky. Matrix factorization techniques for recommender systems. *Computer*, 42(8):30–37, 2009.
18. Suvash Sedhain, Aditya Krishna Menon, Scott Sanner, and Lexing Xie. Autorec: Autoencoders meet collaborative filtering. In *Proceedings of the 24th international conference on World Wide Web*, pages 111–112, 2015.
19. WU CHEN, Lei, HONG Le, and Richang. Revisiting graph based collaborative filtering: A linear residual graph convolutional network approach. In *Proceedings of the AAAI conference on artificial intelligence*, pages 27–34, 2020.
20. Yonghui Yang, Le Wu, Richang Hong, Kun Zhang, and Meng Wang. Enhanced graph learning for collaborative filtering via mutual information maximization. In *Proceedings of the 44th international ACM SIGIR conference on research and development in information retrieval*, pages 71–80, 2021.
21. Tiansheng Yao, Xinyang Yi, Derek Zhiyuan Cheng, Felix Yu, Ting Chen, Aditya Menon, Lichan Hong, Ed H Chi, Steve Tjoa, Jieqi Kang, et al. Self-supervised learning for large-scale item recommendations. In *Proceedings of the 30th ACM international conference on information & knowledge management*, pages 4321–4330, 2021.